Mechanism of phase splitting in two coupled groups of suprachiasmatic-nucleus neurons

Changgui Gu,[1] Jianxiong Wang,[1] Jiaxiang Wang,[2] and Zonghua Liu[1,*]

[1]*Institute of Theoretical Physics and Department of Physics, East China Normal University, Shanghai, 200062, China*

[2]*State Key Laboratory of Precision Spectroscopy, East China Normal University, Shanghai, 200062, China*

(Received 31 October 2010; revised manuscript received 20 March 2011; published 27 April 2011)

The phase-splitting behavior of coupled suprachiasmatic-nucleus neurons has been observed in many mammals, and its mechanism is still not completely understood. Based on our previous work [C. Gu, J. Wang, and Z. Liu, Phys. Rev. E **80**, 030904(R) (2009)] on the free-running periods of neurons in the suprachiasmatic nucleus, we present here a modified Goodwin oscillator model to explain the mechanism of phase splitting. In contrast to the previous phase model, the modified Goodwin oscillator model contains the information on both the phase and amplitude and, thus, can show more features than the purely phase model, including all three behaviors of synchronization, phase splitting, and amplitude death and the distributed periodicity in the regions of synchronization and phase splitting, etc. An analytic phase model is extracted from the modified Goodwin oscillator model to explain the dependence of periodicity on the parameters. Moreover, both the modified Goodwin oscillator model and the analytic phase model show that the ensemble frequency can be enhanced or reduced by the time delay.

DOI: 10.1103/PhysRevE.83.046224 PACS number(s): 05.45.Xt, 87.18.Sn

I. INTRODUCTION

Rhythm is a long-standing problem for people to understand the biological activities, such as the effects of sight, sound, touch, smell, and taste in almost all plants and animals [1], hence, deserving extensive studies [2–6]. Most of the rhythms are closely related to the 24-h circadian period of sunlight such as the insect emergence, roosters crowing, and sleep-waking behavior, etc. Through intense studies, it has been found that the rhythm of mammals is controlled by the suprachiasmatic nucleus (SCN) of the hypothalamus, i.e., a central circadian clock in mammals [7–14]. The SCN is composed of about 20 000 neurons and is in charge of receiving light signals from the retina and then controlling the circadian rhythms. Thus, the fundamental function of the SCN is to transmit time-of-day information to the rest of the body. To implement this task, each SCN neuron has a molecular pacemaker, which can be modeled by the Goodwin oscillator with a negative transcription-translation feedback loop [15]. The pacemaker will produce an output signal such as a change in neuronal excitability or neurotransmitter production. The output signal can be communicated to other brain regions that directly or indirectly regulate activity at the system level [16]. The interaction among the SCN oscillators is through the neurotransmitter and can produce time-of-day dependent changes in the properties of the SCN as a whole, i.e., the rhythm.

On the other hand, it would be interesting to ask what will happen if the 24-h circadian period of sunlight is absent. It is pointed out that exposure to constant light may disrupt overt rhythms somehow and it induces circadian arrhythmicity in mammals and other species [17,18]. Two kinds of consequences can be observed. The first one is that the free-running periods will deviate from the 24-h circadian period and scatter roughly in the range between 20 and 28 h for different species. The second one is that the SCN neurons could double their frequency by spontaneously splitting into two subgroups, each subgroup oscillating with common frequency but now in antiphase, called phase splitting. To explain the mechanism of free running, several approaches and models have been presented [2,19–23]. It is revealed that the reason for different free-running periods is because of the competition between the desynchronizing effect caused by the constant light and the coupling among the oscillators, which can compensate the desynchronizing effect of the dispersion of intrinsic frequencies. Recently, we have also studied this problem [24]. We find that both the coupling strength and its distribution can influence the free-running period, and the free-running period is inversely proportional to the dispersion of couplings.

For the phase splitting, there are evidences to show that rodents such as hamsters will show phase-splitting behaviors if they are exposed for several weeks to constant light [17,25–29]. For example, for arctic ground squirrels under constant light, their activity bands split into two clear bands and the animals run with two different circadian periods with a phase difference of 180° [26–28]. For golden hamsters housed in constant light after two months, their single daily bout of locomotion activity dissociates into two components that become stably coupled about 12 hours apart [25]. This problem recently has been addressed by Indic *et al*., wherein two groups of phase oscillators are used to simulate the neurons in the left and right clock nuclei cycle [18]. They constructed a modified Kuramoto phase model containing the contribution of time delay to show that the phase splitting can show up from two coupled groups of phase oscillators. This kind of phase model fits for huge assemblies of oscillatory elements with natural frequencies, and is thus a general approach. Note that the phase model is only a simplification of the SCN oscillators where only the message on rotation remains. It is pointed out that the amplitude of SCN oscillators is also important as it influences the communication among the SCN oscillators [2,20,24,30]. Thus, the phase splitting of SCN oscillators may also be related to the amplitude of the oscillator. In this sense, it is

*zhliu@phy.ecnu.edu.cn

interesting and necessary to reveal the mechanism of phase splitting directly from the SCN oscillators, in contrast to its simplified phase model. To the best of our knowledge, this problem has not been addressed so far and is thus the purpose of this paper.

In this paper, we first present a modified Goodwin oscillator model to show the existence of phase splitting in two coupled groups of SCN oscillators. By choosing the sets of coupling weights from the same group, a different group, and the part due to time delay, we show that the collective behaviors may be synchronization, antisynchronization, and phase splitting, and even amplitude death [31,32]. We further reveal that, in the regions of synchronization and phase splitting, the period of coupled SCN neurons depends on the coupling weight from the part of time delay. Then, we consider the influence of nonidentity of oscillators and find that the observed collective behaviors are robust to the diversity from both the nonidentical oscillators and the coupling strength distribution. After that, we present an analytic phase model to explain the periodic dependence of coupled SCN neurons on the weight from the delay part, which is based on our previous work [24]. Finally, we make a brief summary.

II. A MODIFIED GOODWIN OSCILLATOR MODEL FOR PHASE SPLITTING

The Goodwin oscillator model was presented to simulate circadian rhythms in SCN cells [2,20,30]. In this model, within each clock cell, a clock gene mRNA (x) produces a clock protein (y) which, in turn, activates a transcriptional inhibitor (z). The latter inhibits the transcription of the clock gene, closing a negative feedback loop. The interaction among the SCN cells is through a neuropeptide denoted by V, induced by the activation of x. The mean-field levels of the neuropeptide (F) then act as a synchronizing factor and are added as an independent term in the transcription rate of x. To explain the diversity of the free-running period of mammals, we recently reconsidered this model [24]. Based on the fact that the individual neurons in SCN are not identical with the same period, we assumed that their coupling strengths are different and satisfy a distribution. Thus, we obtained the following model:

$$\begin{aligned}
\dot{x}_i &= \alpha_1 \frac{k_1^n}{k_1^n + z_i^n} - \alpha_2 \frac{x_i}{k_2 + x_i} + \alpha_c \frac{g_i F}{k_c + g_i F}, \\
\dot{y}_i &= k_3 x_i - \alpha_4 \frac{y_i}{k_4 + y_i}, \\
\dot{z}_i &= k_5 y_i - \alpha_6 \frac{z_i}{k_6 + z_i}, \\
\dot{V}_i &= k_7 x_i - \alpha_8 \frac{V_i}{k_8 + V_i}, \quad i = 1,2,\ldots,N \\
F &= \frac{1}{N} \sum_{i=1}^{N} V_i,
\end{aligned} \tag{1}$$

where x_i, y_i, and z_i constitute a negative feedback loop in the clock cell$-i$. The intercellular coupling is implemented through the global neurotransmitter F, which acts as a mean field. The coupling strength g_i describes the sensitivity of the individual SCN oscillator to the neurotransmitter and satisfies a distribution. Following Ref. [20], we take the parameters as $\alpha_1 = 0.7nM/h$, $k_1 = 1nM$, $n = 4$, $\alpha_2 = 0.35nM/h$, $k_2 = 1nM$, $k_3 = 0.7/h$, $\alpha_4 = 0.35nM/h$, $k_4 = 1nM$, $k_5 = 0.7/h$, $\alpha_6 = 0.35nM/h$, $k_6 = 1nM$, $k_7 = 0.35/h$, $\alpha_8 = 1nM/h$, $k_8 = 1nM$, $\alpha_c = 0.4nM/h$, and $k_c = 1nM$. For nonidentical oscillators, their different periods can be implemented by dividing the parameters α_1, α_2, k_3, α_4, k_5, α_6, k_7, and α_8 by a scaling factor τ_i [20,30]. Reference [24] showed that the results obtained from the constant $\tau_i = 1$ also work for the case with distributed τ_i.

We now modify Eq. (1) to fit for the case of phase splitting. Following Ref. [24], for simplicity, we also limit our discussion to the case of scaling factor $\tau_i = 1$ but let the distributed g_i reflect the property of nonidentity of individual SCN oscillators. To discuss the phase splitting, we divide the oscillators into two groups, representing the left and right SCN clock cells of the hypothalamus. Suppose the first group has N_1 oscillators and the second group has N_2 oscillators with $N_1 + N_2 = N$. Considering that the mean field F will be the same in one group and different in another group, we let the F in Eq. (1) be F_1 for the first group and F_2 for the second group. As a necessary condition to observe the phase splitting in the long time constant light, we need to consider the effect of constant light to get the correct expression of $F_{1,2}$.

In general, the circadian oscillators in the SCN couple together to generate a circadian output signal to regulate the day-night rhythm. Then, the output signal feeds back to alter the phase of the SCN itself [33], and the presence of light can modify the strength and timing of this feedback signal [34]. Considering that the feedback signal will have some time delay, the constant light will make this time delay become larger and then weaken the coupling among the SCN oscillators. This effect of weakening coupling can be also implemented by another way of increasing light in the light-dark (LD) cycle, where light represents the daytime and dark the nighttime. It was pointed out that, as increasing light may result in a transition from a rhythmic to an arrhythmic behavior, the coupling strength may be inversely dependent on the light intensity, i.e., the larger the light intensity, the weaker the coupling [35,36]. We only focus here on the effect of constant light. Compared with the LD cycle, the constant light can be considered as a light-light (LL) cycle. That is, the dark in LD is replaced by the light in LL, which is the source for the constant light to contribute to the $F_{1,2}$. We may assume that the time delay in $F_{1,2}$ is very large. An evidence to support this assumption is that the reference [18] took the time delay as large as 12 h, and also theoretically proved that the phase splitting can be observed only when the time delay is in between $T/4$ and $3T/4$ with $T = 24$ h. Motivated by this work, we think that a contribution with time delay should be included into $F_{1,2}$ to reflect the effect of constant light. Therefore, we assume that $F_{1,2}$ can be expressed as

$$\begin{aligned}
F_1 &= \frac{a}{N} \sum_{i=1}^{N_1} V_i + \frac{b}{N} \sum_{i=N_1+1}^{N} V_i + \frac{c}{N} \sum_{i=1}^{N} V_{i,-\tau}, \\
F_2 &= \frac{b}{N} \sum_{i=1}^{N_1} V_i + \frac{a}{N} \sum_{i=N_1+1}^{N} V_i + \frac{c}{N} \sum_{i=1}^{N} V_{i,-\tau},
\end{aligned} \tag{2}$$

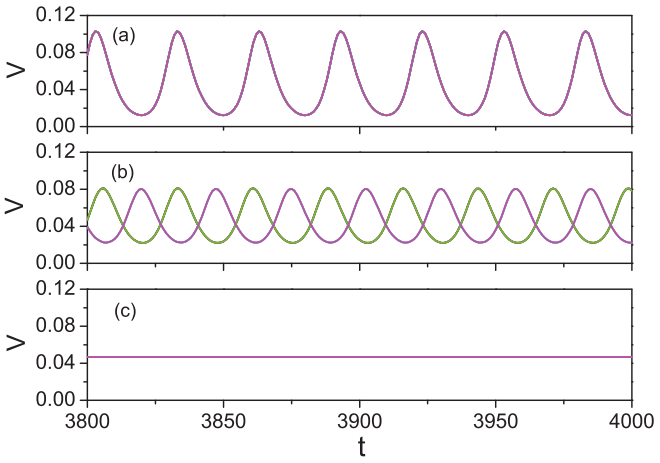

FIG. 1. (Color online) The collective behaviors for the coupling strength $g = 0.5$, the time delay $\tau = 11$ h, and the oscillator numbers $N_1 = N_2 = N/2 = 50$ where the unit of t is hours and (a) represents the case of synchronization with $a = 1.64$ and $b = 0.32$; (b) represents the case of antisynchronization with $a = 1.64$ and $b = 0.16$; and (c) represents the case of amplitude death with $a = 1.16$ and $b = 0.28$.

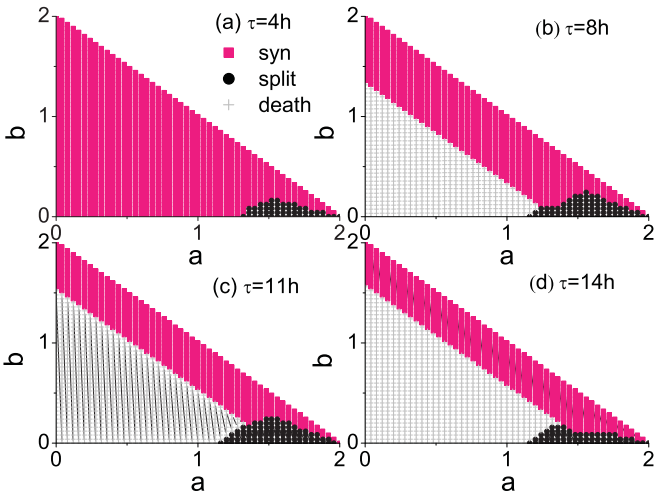

FIG. 2. (Color online) Phase diagram in the ab plane with $g = 0.5$ and $N_1 = N_2 = N/2 = 50$ where the "squares", "circles", and "pluses" denote the synchronization, phase splitting, and amplitude death, respectively, and (a)–(d) represent the cases with time delay $\tau = 4$, 8, 11, and 14 h, respectively.

where the parameters a, b, and c represent the coupling weights from the same group, a different group, and the part due to time delay, respectively, and satisfy the relationship

$$(a + b)/2 + c = 1. \tag{3}$$

Thus, the first equation of (1) can be rewritten as

$$\begin{aligned} \dot{x}_i &= \alpha_1 \frac{k_1^n}{k_1^n + z_i^n} - \alpha_2 \frac{x_i}{k_2 + x_i} + \alpha_c \frac{g_i F_1}{k_c + g_i F_1}, \\ & i = 1,2,\ldots,N_1 \\ \dot{x}_i &= \alpha_1 \frac{k_1^n}{k_1^n + z_i^n} - \alpha_2 \frac{x_i}{k_2 + x_i} + \alpha_c \frac{g_i F_2}{k_c + g_i F_2}, \\ & i = N_1 + 1, N_1 + 2, \ldots, N \end{aligned} \tag{4}$$

and the other equations in (1) remain unchanged. This is the modified Goodwin oscillator model for phase splitting and will be used in this paper. It is easy to see from Eq. (2) that, when the two groups merge into one with $a = b$ and $\tau = 0$, we have $F_1 = F_2 = F$, i.e., Eq. (2) returns to the previous F in Eq. (1).

In numerical simulations, we take $N = 100$ and $N_1 = N_2 = 50$. Following Ref. [18], we make numerical integrations by the fourth-order Runge-Kutta method with a time step of 0.1 h. The initial conditions are chosen randomly from (0,1). We first consider the case of identical oscillators with all the $g_i = g = 0.5$. We find that, after the transient process, the oscillators from the two groups will show some interesting behaviors such as synchronization, antisynchronization, and even amplitude death. As the antisynchronization has the same phase in one group and a phase difference of 180° between the two groups, it is in fact the phase splitting. Figure 1 shows the typical results for six randomly chosen oscillators from the two groups where (a)–(c) represent the synchronization, antisynchronization, and amplitude death, respectively.

To show how the collective behaviors depend on the coupling weights a, b, and c, it is necessary to figure out the phase diagram. For this purpose, we define the amplitude death as the states with $V_i^{\max} - V_i^{\min} < 0.01$, where $V_i^{\max}$ ($V_i^{\min}$) represents the maximum (minimum) of V_i. Figure 2 shows the phase diagram of the synchronization, antisynchronization, and amplitude death for $N_1 = N_2 = N/2 = 50$ and different time delays, respectively. It is easy to see that the antisynchronization occurs only in the area with larger a and smaller b in all four panels, while the synchronized area is very large in Fig. 2(a) and gradually decreases in 2(b)–2(d), indicating the dependence of the collective behaviors on the time delay. It is also noticed that the boundary regions in Fig. 2 are co-existing with dynamical regimes (synchronization, split, death) where the collective behavior depends on the initial conditions. Except for these co-existing regimes, our numerical simulations show that the behaviors in other regimes are robust to the initial conditions.

To see how the size of the ensemble influences the collective behaviors, we have checked the cases of different N and found that they are similar to Fig. 2, indicating the robustness to N. Thus, in the following, we will only focus on the case of $N = 100$, i.e., $N_1 = N_2 = N/2 = 50$.

We would like to provide some explanation for the observed collective behaviors. For the amplitude death, we have $V_{i,-\tau} = V_i = \text{const}$. In this case, the part with time delay in the coupling term F has the same function with the other two parts and, thus, the delay has no influence on the system. While V_i is in the oscillatory status, we generally have $V_{i,-\tau} \neq V_i$. That is, the delay part $V_{i,-\tau}$ will have a different phase with the nondelay part V_i and thus have a different function. Suppose the oscillation solution exists in the range $0 < c < c_0(b)$ where c_0 depends on b. As both the term with b and the term with c in Eq. (2) have a different phase from the term with a in Eq. (2), their mixture can be considered as a perturbation to the term with a in $F_{1,2}$. In this perturbation, the term with c comes from the feedback of output signal and is thus not very large. For the case of larger b, the perturbation is mainly controlled by the term with b and, thus, c can

be approximately considered as independent of b. In this situation, $c = 0$ corresponds to the line $a + b = 2$, while $c = c_0$ corresponds to the line $a + b = 2(1 - c_0)$. That is, the range for the oscillation solution is $2(1 - c_0) < a + b < 2$. In the ab plane, both the lines $a + b = 2$ and $a + b = 2(1 - c_0)$ have the same slope -1 and the oscillation region is the area between these two lines. As the $V_{i,-\tau}$ is inconsistent with V_i in the oscillatory region, the threshold c_0 will be closely related to the delay τ, confirming the results observed in Figs. 2(a)–2(d). When $a + b$ is beyond this area, i.e., $c > c_0$, the delay term $\frac{c}{N}\sum_{i=1}^{N} V_{i,-\tau}$ may be strong enough to make F_i tend to uniform and thus reduce its oscillation amplitude and gradually make it become a constant, i.e., reach the amplitude death. However, when b is small, both the term with b and the term with c in Eq. (2) will provide an equal contribution to the perturbation. Then, c_0 can not be considered as independent of b, i.e., $c_0 = c_0(b)$, which results in the speckles in the death regime in Fig. 2. Theoretically, c_0 can be considered as a balance between the first term with normal phase and the perturbation with delayed phase in Eq. (2). The system will be oscillation when the first term can suppress the perturbation; otherwise, the system will be the amplitude death.

The oscillation region of $0 < c < c_0(b)$ can be further divided into two parts. One is the synchronized region and the other is the antisynchronized or phase-splitting region. When $F_{1,2}$ is mainly contributed by the coupling part from the oscillators of the same group, i.e., $a \gg b$, the contribution from a different group can be considered as a perturbation and thus the two groups will be relatively independent. In this case, F_1 may have a significant difference from F_2, resulting in the fact that the two groups may have different status, i.e., antisynchronization. When b is not very small, F_1 and F_2 will tend to be the same and thus result in the synchronization status.

Furthermore, we find that even in the regions of synchronization and phase splitting, the dynamical behaviors are not always the same. That is, their periodicity will change with the parameters a and b. Figure 3 shows the different periodic bands where 3(a)–3(d) represent the cases with time delay

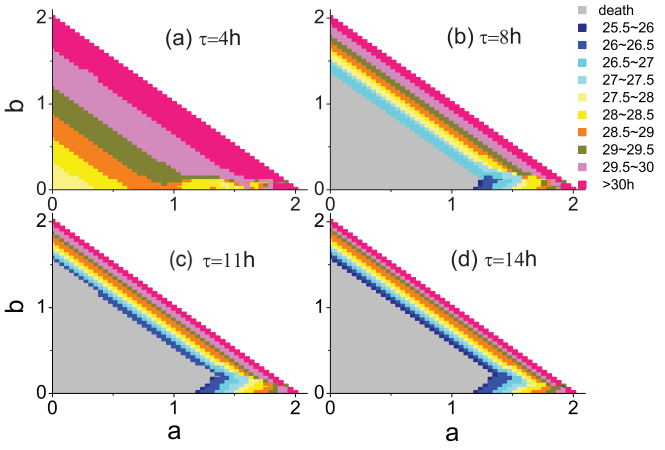

FIG. 3. (Color online) The periodicity corresponding to Fig. 2 where the different colors denote different periods, respectively, and (a)–(d) represent the cases with time delay $\tau = 4$, 8, 11, and 14 h, respectively.

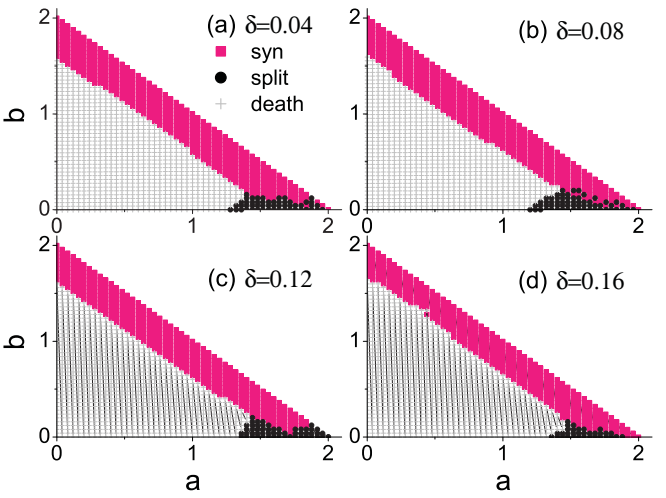

FIG. 4. (Color online) Phase diagram in the ab plane with $\tau = 14$ h and $N_1 = N_2 = N/2 = 50$ where the "squares", "circles", and "pluses" denote the synchronization, phase splitting, and amplitude death, respectively, and (a)–(d) represent the cases with the standard deviation $\delta = 0.04$, 0.08, 0.12, and 0.16, respectively.

$\tau = 4$, 8, 11, and 14 h, respectively. Considering that each line with slope -1 in all the panels of Fig. 3 represents a fixed value of c in the synchronization region, we conclude that the period of coupled SCN oscillators in the synchronization region is determined by the weight c. We will analytically explain this in the next section.

We now turn to the case with distributed coupling strengths. We consider the case of Gaussian distribution with the average $\langle g_i \rangle = 0.5$ and deviation δ. We find that the observed collective behaviors are robust to the distribution. Figure 4 shows the results of the delay $\tau = 14$ h where 4(a)–4(d) represent the situations of $\delta = 0.04$, 0.08, 0.12, and 0.16, respectively. It is easy to see that the four panels in Fig. 4 are very similar, indicating the robustness of the synchronized region to the distribution of coupling strengths. However, we find that the periodicity is influenced by the distribution. Figure 5 shows the corresponding periods. From the four panels of Fig. 5, we see that the periods tend to decrease with the increase of the deviation δ.

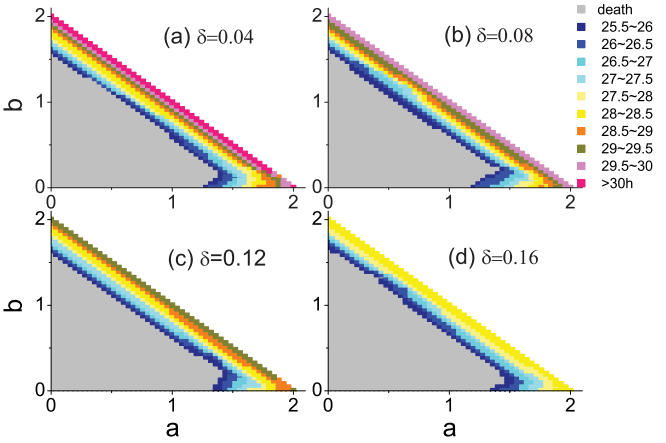

FIG. 5. (Color online) The periodicity corresponding to Fig. 4 where the parameters are the same with Fig. 4.

III. AN ANALYTIC PHASE MODEL

In Ref. [24], we observed that larger g_i corresponds to larger T or, equivalently, small frequency ω_i for individual oscillators. Based on this observation, we suggested that the intrinsic frequency of the ith oscillator can be assumed as $\omega_i = \omega_0 - dg_i$ with constants ω_0 and d. To consider the dispersion of coupling, we assumed that the coupling g_i satisfy a normal distribution with average $\langle g \rangle$ and standard variation σ. Thus, we obtained a phase model [24]

$$\dot{\theta}_i = \omega_0 - dg_i + \frac{g_i}{N}\sum_{j=1}^{N}\sin(\theta_j - \theta_i) \tag{5}$$

with $1 \leqslant i, j \leqslant N$. This model corresponds to Eq. (1). To use it to explain the phase splitting, we need to make some modification to it. According to the expression of $F_{1,2}$ in Eq. (2), we modify Eq. (5) into

$$\dot{\theta}_i = \omega_0 - dg_i + \frac{g_i}{N}\left[a\sum_{j=1}^{N_1}\sin(\theta_j - \theta_i) + b\sum_{j=1+N_1}^{N}\sin(\theta_j - \theta_i) + c\sum_{j=1}^{N}\sin(\theta_{j,-\tau} - \theta_i)\right] \tag{6}$$

for the first group and

$$\dot{\theta}_i = \omega_0 - dg_i + \frac{g_i}{N}\left[a\sum_{j=1+N_1}^{N}\sin(\theta_j - \theta_i) + b\sum_{j=1}^{N_1}\sin(\theta_j - \theta_i) + c\sum_{j=1}^{N}\sin(\theta_{j,-\tau} - \theta_i)\right] \tag{7}$$

for the second group, where the parameters a, b, and c still have the meaning of coupling weights from the same group, a different group, and the part due to time delay, respectively, and satisfy the relation (3). Equations (6) and (7) are our analytic phase model.

To obtain the solution of Eqs. (6) and (7), we first focus on the case of identical oscillators with intrinsic frequency ω, coupling strength g, and oscillator numbers $N_1 = N_2 = N/2$. We must point out that different from the modified Goodwin model (4), the phase models (6) and (7) do not have any oscillation amplitude but only phase, thus, we will not observe the amplitude death again. That is, we will only observe the synchronization and antisynchronization. Based on the observed results, we can figure out the dependence of periodicity on the parameters a and b or the parameter c.

When the coupled oscillators are synchronized, they will have a common frequency Ω. Letting $t = 0$ be the time for the oscillators to be synchronized, the solution of Eqs. (6) and (7) can be expressed as

$$\theta_i = \Omega t + \theta_{i0} \tag{8}$$

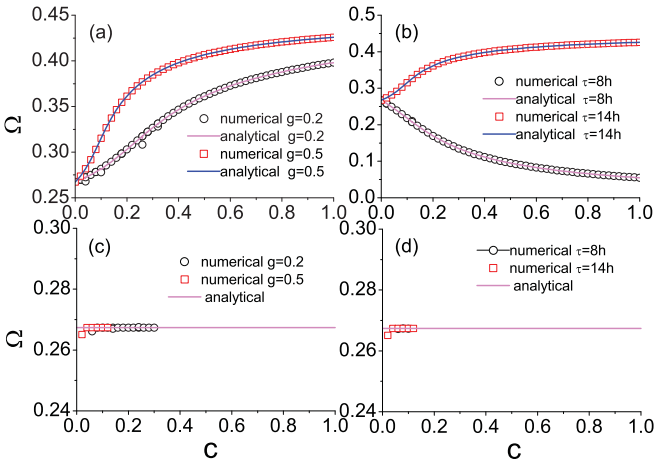

FIG. 6. (Color online) The dependence of frequency Ω on the parameters c, g, and τ with $N_1 = N_2 = N/2 = 50$. (a) and (b) represent the case of synchronization with $\tau = 14$ h in (a) and $g = 0.5$ in (b). (c) and (d) represent the case of phase splitting with $\tau = 14$ h in (c) and $g = 0.5$ in (d).

for all the oscillators, where θ_{i0} is the phase of the oscillator i right before synchronization. Substituting Eq. (8) into (6), we have

$$\Omega = \omega - dg + \frac{g}{N}\left[a\sum_{j=1}^{N_1}\sin\left(\theta_{j_0} - \theta_{i_0}\right) + b\sum_{j=N_1+1}^{N}\sin\left(\theta_{j_0} - \theta_{i_0}\right) + c\sum_{j=1}^{N}\sin\left(\theta_{j_0} - \theta_{i_0} - \Omega\tau\right)\right] \tag{9}$$

for the group-1. The similar form can be obtained for the group-2. Taking the average to all the N oscillators, we have

$$\Omega = \omega - dg + \frac{g}{N^2}\left[c\sum_{i,j=1}^{N}\sin\left(\theta_{j_0} - \theta_{i_0} - \Omega\tau\right)\right] = \omega - dg - \frac{cg}{N^2}\sin\Omega\tau\sum_{i,j=1}^{N}\cos\left(\theta_{j_0} - \theta_{i_0}\right). \tag{10}$$

For the case of identical oscillators, we especially have $\theta_{j_0} = \theta_{i_0}$ and thus

$$\Omega = \omega - dg - cg\sin\Omega\tau. \tag{11}$$

Therefore, the frequency Ω is determined by the parameters c, g, and τ, which explains the results observed in Figs. 3 and 5. To check it numerically from the analytical models (6) and (7), we let $d = 0$ and $\omega = 2\pi/T$, where $T = 23.5$ h is the free period of a single SCN oscillator of Eq. (1) [20]. Figure 6(a) shows how Ω changes with the parameter c for $\tau = 14$ h where the "circles" and "squares" represent the numerical results for the cases of $g = 0.2$ and 0.5, respectively, and the "red line" and "black line" are the corresponding theoretical results from Eq. (11). Obviously, the numerical results completely agree with the theoretical predictions. This result can be explained by Eq. (11) as follows. In the observed range of Ω in Fig. 6(a), we have $\Omega\tau > \pi$ and, thus, $\sin\Omega\tau < 0$, indicating that Ω

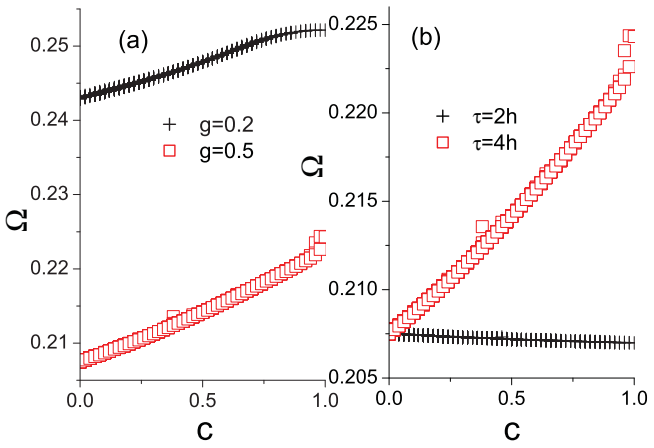

FIG. 7. (Color online) The results directly from the modified Goodwin models (1)–(4) with $N_1 = N_2 = N/2 = 50$. (a) and (b) represent the case of synchronization with $\tau = 4$ h in (a) and $g = 0.5$ in (b).

increases with c. Moreover, $|\sin\Omega\tau|$ will nonlinearly increase with Ω for $\pi < \Omega\tau < 3\pi/2$ and then decrease with Ω for $\Omega\tau > 3\pi/2$. Thus, Fig. 6(a) is a combined effect from the two factors of both c and $\sin\Omega\tau$, which is nothing but just the prediction of Eq. (11). Figure 6(b) shows how Ω changes with c for $g = 0.5$ where the "circles" and "squares" represent the cases of $\tau = 8$ and 14 h, respectively, and the "red line" and "black line" are the corresponding theoretical results from Eq. (11). This result can be also explained by Eq. (11). In the observed range of Ω in Fig. 6(b), we have $\Omega\tau < 0$ for the case of $\tau = 14$ h and $\Omega\tau > 0$ for the case of $\tau = 8$ h, indicating that Ω will increase with c for $\tau = 14$ h but decrease with c for $\tau = 8$ h. Combining the factors of both c and $\sin\Omega\tau$, we can understand the observed phenomenon in Fig. 6(b).

To check the relationship between the analytic models (6) and (7) and the modified Goodwin models (1)–(4), we calculate the relationship between Ω and c directly from the modified Goodwin model. Figure 7 shows the results where (a) shows how Ω changes with the parameter c for $\tau = 4$ h where the "pluses" and "squares" represent the numerical results for the cases of $g = 0.2$ and 0.5, respectively, and (b) shows how Ω changes with c for $g = 0.5$ the "pluses" and "squares" represent the cases of $\tau = 2$ and 4 h, respectively. Comparing Figs. 7(a) and 7(b) with Figs. 6(a) and 6(b), respectively, we see that their varying tendencies are similar although their values are different, indicating their qualitative agreement.

When the coupled oscillators are antisynchronized or phase splitting, they will also have a common frequency Ω but a phase difference of π between the two groups. Letting $t = 0$ be the time for the oscillators to reach the phase splitting, the solution of Eqs. (6) and (7) can be expressed as

$$\theta_i = \Omega t + \theta_{i0} \tag{12}$$

for the group-1 with $i = 1, 2, \ldots, N_1$ and

$$\theta_i = \Omega t + \theta'_{i0} + \pi \tag{13}$$

for the group-2 with $i = N_1 + 1, N_1 + 2, \ldots, N$. Substituting Eqs. (12) and (13) into (6), we obtain

$$\begin{aligned}\Omega = \omega - dg + \frac{g}{N}\Bigg[& a\sum_{j=1}^{N_1}\sin\left(\theta_{j_0} - \theta_{i_0}\right) \\ & + b\sum_{j=N_1+1}^{N}\sin\left(\theta'_{j_0} - \theta_{i_0} + \pi\right) + c\sum_{j=1}^{N_1}\sin\left(\theta_{j_0} - \theta_{i_0} - \Omega\tau\right) \\ & + c\sum_{j=N_1+1}^{N}\sin\left(\theta'_{j_0} - \theta_{i_0} - \Omega\tau + \pi\right)\Bigg]\end{aligned} \tag{14}$$

for the group-1. The similar form can be obtained for the group-2. Taking the average to all the N oscillators, we have

$$\begin{aligned}\Omega &= \omega - dg + \frac{g}{N^2}\Bigg[c\sum_{i,j=1}^{N_1}\sin\left(\theta_{j_0} - \theta_{i_0} - \Omega\tau\right) + c\sum_{i,j=N_1+1}^{N}\sin\left(\theta'_{j_0} - \theta'_{i_0} - \Omega\tau\right) \\ &\quad - c\sum_{i=1}^{N_1}\sum_{j=N_1+1}^{N}\sin\left(\theta_{i_0} - \theta'_{j_0} - \Omega\tau\right) - c\sum_{i=1}^{N_1}\sum_{j=N_1+1}^{N}\sin\left(\theta'_{j_0} - \theta_{i_0} - \Omega\tau\right)\Bigg] \\ &= \omega - dg - \frac{cg}{N^2}\sin\Omega\tau\Bigg[\sum_{i,j=1}^{N_1}\cos\left(\theta_{j_0} - \theta_{i_0}\right) + \sum_{i,j=N_1+1}^{N}\cos\left(\theta'_{j_0} - \theta'_{i_0}\right) \\ &\quad - \sum_{i=1}^{N_1}\sum_{j=N_1+1}^{N}\cos\left(\theta_{i_0} - \theta'_{j_0}\right)\Bigg].\end{aligned} \tag{15}$$

For the case of identical oscillators, we especially have $\theta_{j_0} = \theta_{i_0} = \theta'_{j_0} = \theta'_{i_0}$ and, thus,

$$\Omega = \omega - dg. \tag{16}$$

Therefore, the frequency Ω is independent of the parameters c, g, and τ for the case of $d = 0$. Figures 6(c) and 6(d) show the results from both the numerical simulations of the models (6) and (7) and the theoretical prediction of Eq. (16) in the region

of phase splitting. Obviously, they confirm each other well. Furthermore, from Figs. 6(c) and 6(d), we see that the phase splitting exists only in a small range of c, which theoretically explains the results in Fig. 2.

As in Figs. 7(a) and 7(b), it is necessary to get corresponding Figs. 6(c) and 6(d) directly from the modified Goodwin models (1)–(4). However, we surprisingly find that we can not obtain a constant Ω for varying c. This can be understood from Fig. 2. Notice that the phase-splitting areas in Figs. 2(b)–2(d) are irregular, indicating that all three parameters a, b, and c are competitive to make a phase splitting. The resulted $F_{1,2}$ will also be irregular and thus influences the frequency of the system and results in a varying Ω in phase splitting, which can not be given by the analytic model.

For the case of distributed g_i, we go back to the Eqs. (6) and (7). By performing the similar derivative process, we obtain

$$\Omega = \omega - d\langle g_i\rangle - \frac{c\langle g_i\rangle}{N^2}\sin\Omega\tau\sum_{i,j=1}^{N}\cos\left(\theta_{j_0}-\theta_{i_0}\right)+\xi \quad (17)$$

for the region of synchronization and

$$\Omega = \omega - d\langle g_i\rangle - \frac{c\langle g_i\rangle}{N^2}\sin\Omega\tau\left[\sum_{i,j=1}^{N_1}\cos\left(\theta_{j_0}-\theta_{i_0}\right) + \sum_{i,j=N_1+1}^{N}\cos\left(\theta'_{j_0}-\theta'_{i_0}\right) - \sum_{i=1}^{N_1}\sum_{j=N_1+1}^{N}\cos\left(\theta_{i_0}-\theta'_{j_0}\right)\right]+\xi \quad (18)$$

for the region of phase splitting, where $\langle g_i\rangle$ represents the average of g_i and ξ denotes the fluctuation. Comparing Eqs. (17) and (18) with Eqs. (10) and (15), respectively, we see that they have similar forms, indicating the robustness to the distribution of coupling strengths and the nonidentity of oscillators.

IV. DISCUSSIONS AND CONCLUSIONS

In this paper, we have introduced both the modified Goodwin models (1)–(4) and the analytic models (6) and (7). Comparing these two models, we find that the modified Goodwin model can show more features than the analytic model. The first feature is that the modified Goodwin model can show the amplitude death, while the analytic model can not. It is reported that, under bright light, the endogenous circadian amplitude will be suppressed and results in the loss of rhythmicity, i.e., the amplitude death is related to the loss of rhythmicity in animal or human [37,38]. The second feature is that, in describing the phase splitting, the analytic model shows a constant Ω for varying c while the modified Goodwin model shows a varying Ω. The third feature is that, in describing the synchronization, the analytic model is qualitatively but not quantitatively consistent with the modified Goodwin model. These differences make us believe that the modified Goodwin model with information of amplitude can explain more circadian rhythmic features than a phase model without the information of amplitude.

In the modified Goodwin model, the phase space can be divided into three different regions by the coupling weight parameters a, b, and c. For each fixed delay τ, there is a threshold c_0. The death and oscillatory status are bordered by the value of c_0. It is death for $c > c_0$ and oscillatory for $c < c_0$. In the oscillatory region, the collective behaviors can be further divided into synchronization and phase splitting, which is distinguished by the relative weights between a and b. When $a \gg b$, i.e., b close to zero, F_i is mainly determined by the contribution of the coupling part in a group and the contribution from another group can be considered as a perturbation. In this case, it is possible for the two groups to remain in a different status, i.e., phase splitting. Compared to the previous phase model [18], our modified Goodwin model can show not only the phase splitting, but also the amplitude death and the periodicity in the regions of synchronization and phase splitting.

In conclusion, we have presented a modified Goodwin model to better understand biological phase splitting observed in mammals, such as hamsters. The model distinguishes the contributions from the same group and a different group and considers the factor of constant light by a part with time delay in the coupling. We have revealed that, different from the previous phase model, our model can show all the three typical states observed in mammals, i.e., synchronization, phase splitting, and amplitude death. Furthermore, we find that the delay part will significantly influence the periodicity of coupled SCN oscillators. An analytic phase model has been extracted from the modified Goodwin model to explain the dependence of periodicity on the parameters.

ACKNOWLEDGMENTS

We thank an anonymous referee for helping us to improve the paper and pointing us to the useful references. This work was supported by the NNSF of China under Grants No. 10975053 and No. 10635040, by the East China Normal University under Grant No. 2010027, and by State Key Laboratory of Precision Spectroscopy.

[1] W. L. Koukkari and R. B. Sothern, *Introducing Biological Rhythms* (Springer, New York, 2006).
[2] S. Bernard, D. Gonze, B. Cajavec, H. Herzel, and A. Kramer, PLoS Comput. Biol. **3**, e68 (2007).
[3] A. Ahlgren and F. Halberg, *Cycles of Nature: An Introduction to Biological Rhythms* (National Science Teachers Association, Washington, D.C., 1990).
[4] G. Kurosawa and A. Goldbeter, J. Theor. Biol. **242**, 478 (2006).
[5] C. A. Czeisler *et al.*, Science **284**, 2177 (1999).
[6] M. R. Smith, H. J. Burgess, L. F. Fogg, and C. I. Eastman, PLoS One **4**, e6014 (2009).
[7] R. Y. Moore, J. C. Speh, and R. K. Leak, Cell Tissue Res. **309**, 89 (2002).

[8] D. K. Welsh, D. E. Logothetis, M. Meister, and S. M. Reppert, Neuron **14**, 697 (1995).
[9] S. Honma, W. Nakamura, T. Shirakawa, and K. Honma, Neurosci. Lett. **358**, 173 (2004).
[10] M. H. Hastings and E. D. Herzog, J. Biol. Rhythms **19**, 400 (2004).
[11] T. Kalamatianos, I. Kallo, H. D. Piggins, and C. W. Coen, J. Comp. Neurol. **475**, 19 (2004).
[12] T. Noguchi and K. Watanabe, Brain Res. **1239**, 119 (2008).
[13] H. Albus, M. J. Vansteensel, S. Michel, G. D. Block, and J. H. Meijer, Curr. Biol. **15**, 886 (2005).
[14] L. P. Shearman, M. J. Zylka, D. R. Weaver, L. F. Kolakowski Jr., and S. M. Reppert, Neuron **19**, 1261 (1997).
[15] B. C. Goodwin, Adv. Enzyme Regul. **3**, 425 (1965).
[16] B. H. Miller, E. L. McDearmom, and J. S. Takahashi, *The Mammalian Circadian System: From Genes to Behavior* (Springer-Verlag, Berlin, Heidelberg, 2007).
[17] H. Ohta, S. Yamazaki, and D. G. McMahon, Nat. Neurosci. **8**, 267 (2005).
[18] P. Indic, W. J. Schwartz, and D. Paydarfar, J. R. Soc., Interface **5**, 873 (2008).
[19] H. Daido, Phys. Rev. Lett. **87**, 048101 (2001).
[20] D. Gonze, S. Bernard, C. Waltermann, A. Kramer, and H. Herzel, Biophys. J. **89**, 120 (2005).
[21] J. C. Leloup, D. Gonze, and A. Goldbeter, J. Biol. Rhythms **14**, 433 (1999).
[22] P. Ruoff and L. Rensing, J. Theor. Biol. **179**, 275 (1996).
[23] P. Ruoff, M. Vinsjevik, C. Monnerjahn, and L. Rensing, J. Theor. Biol. **209**, 29 (2001).
[24] C. Gu, J. Wang, and Z. Liu, Phys. Rev. E **80**, 030904(R) (2009).
[25] H. O. de la Iglesia, J. Meyer, A. C. Jr., and W. J. Schwartz, Science **290**, 799 (2000).
[26] C. S. Pittendrigh and S. Daan, J. Comp. Physiol. A **106**, 333 (1976).
[27] C. S. Pittendrigh, Annu. Rev. Physiol. A **55**, 17 (1993).
[28] T. Pavlidis, Bull. Math. Biol. **40**, 675 (1978).
[29] L. Yan, N. C. Foley, J. M. Bobula, L. J. Kriegsfeld, and R. Silver, J. Neurosci. **25**, 9017 (2005).
[30] J. C. W. Locke, P. O. Westermark, A. Kramer, and H. Herzel, BMC Syst. Biol. **2**, 22 (2008).
[31] A. Koseska, E. Volkov, and J. Kurths, Europhys. Lett. **85**, 28002 (2009).
[32] A. Prasad, M. Dhamala, B. M. Adhikari, and R. Ramaswamy, Phys. Rev. E **81**, 027201 (2010).
[33] N. Mrosovsky, Biol. Rev. Camb. Philos. Soc. **71**, 343 (1996).
[34] J. Schaap and J. H. Meijier, Eur. J. Neurosci. **13**, 1955 (2001).
[35] E. Ullner, J. Buceta, A. Diez-Noguera, and J. Garcia-Ojalvo, Biophys. J. **96**, 3573 (2009).
[36] A. Diez-Noguera, Am. J. Physiol. Regul. Integr. Comp. Physiol. **267**, R1118 (1994).
[37] M. E. Jewett, R. E. Kronauer, and C. A. Czeisler, Nature (London) **350**, 59 (1991).
[38] A. T. Winfree, J. Comp. Physiol. **85**, 105 (1973).